SUPPLEMENTAL FIGURES AND LEGENDS

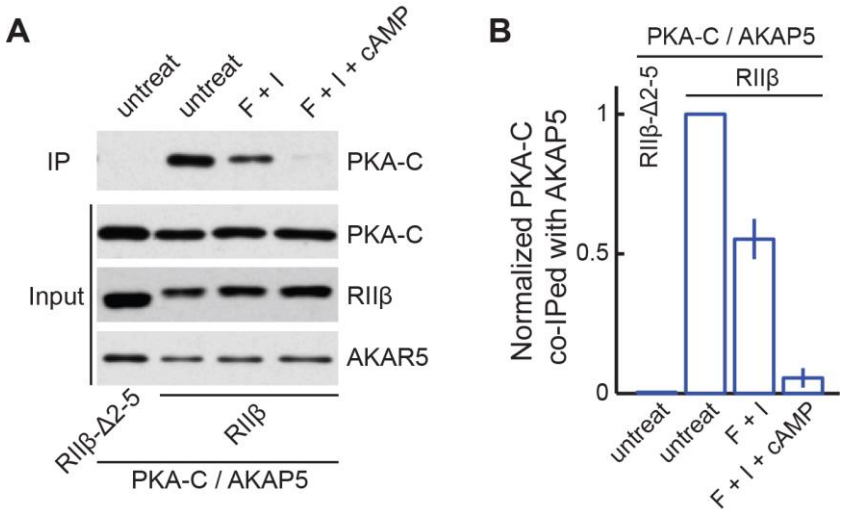

Figure S1. Related to Figure 1. PKA-C dissociates from the PKA-R/AKAP complex in HEK 293 cells upon strong stimulation.

Representative immunoblots (A) and quantifications (B) of co-immunoprecipitation experiment. PKA-C-mCherry and EGFP-AKAP5 were co-transfected with either wildtype or mutant PKA-RIIβ subunit. PKA-C was co-immunoprecipitated with PKA-RIIβ/AKAP5 using an anti-GFP antibody under baseline conditions. This interaction was attenuated to ~ 50% (55 ± 7% of control, n = 4) if the cells were pre-activated by forskolin and IBMX (F + I) and was nearly completely abolished (6 ± 3%, n = 4) if 5 µM Sp-8-pCPT-cAMP was further added to the co-immunoprecipitation reaction.

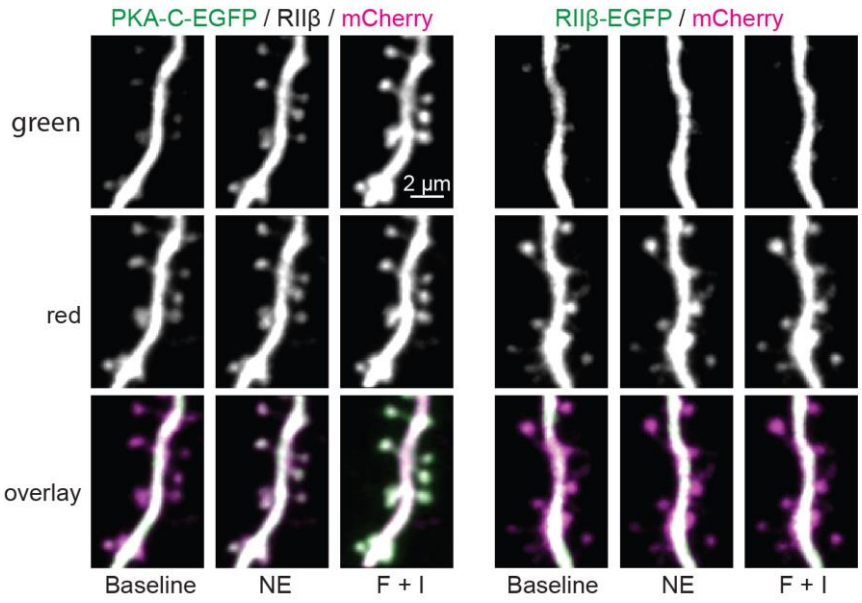

Figure S2. Related to Figure 1. Grayscale and overlaid color images for Figure 1D.

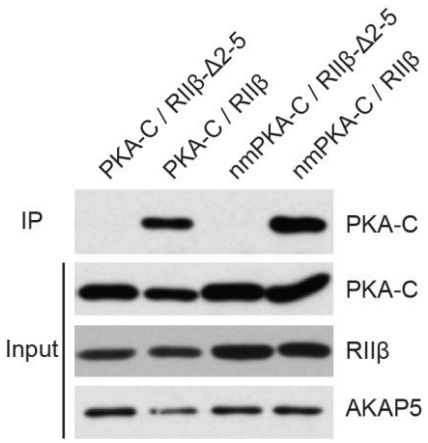

Figure S3. Related to Figure 2. The non-myristoylated mutant of PKA-C still binds to the PKA-RIIβ/AKAP5 complex.

Both wildtype and non-myristoylated PKA-C-mCherry were co-immunoprecipitated with EGFP-AKAP5 using an anti-GFP antibody when co-expressed PKA-RIIβ, but not RIIβ-Δ2-5 that can no longer bind AKAP5.

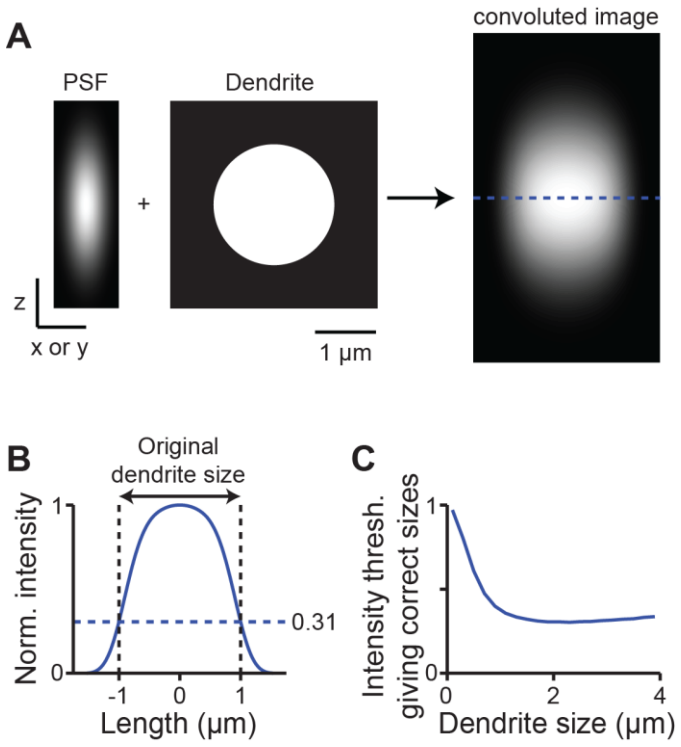

Figure S4. Related to Figure 3. Identifying the edge of a dendrite in a two-photon image.

Two-photon fluorescence microscopes have a finite resolution, as defined by its point spread function (PSF). With a 1.0 NA objective, two-photon PSFs typically have a lateral full width half maximum (FWHM) of ~0.5 μm and a 1.6 μm FWHM in the z dimension. Such a finite resolution limit makes it difficult to determine the exact size and edge of a dendrite. Simulations were performed in order to evaluate the effect of two-photon PSFs in affecting apparent dendrite size. (A) The side view of a simulated two-photon PSF (left). When it was convolved with a 2 μm diameter dendrite (middle), the resulting image looked oval in the side view, and was without a sharp edge (right). (B) The line profile corresponding to the blue line in panel A. When we set a threshold to be 31% of the maximum of the line profile, the resulting lateral size was approximately the original dendrite size. (C) The intensity thresholds at different dendrite sizes that gave the correct dendrite size estimation. For

thick dendrites that were larger than 1.5 μm in diameter, the thresholds were stable to values between 0.3 and 0.35. We therefore used 30% of maximum intensity of the cytosol marker to estimate the edge of experimental dendrites.

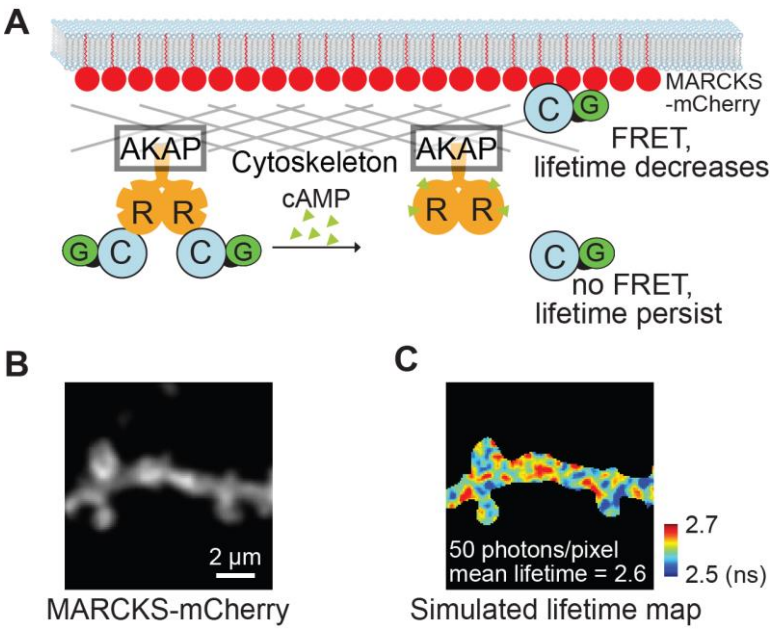

Figure S5. Related to Figure 3. Illustration of the design and noise of the FRET/FLIM experiment in Figure 3C and 3D.

(A) MARCKS-mCherry (red) is expressed so that mCherry is targeted to the plasma membrane and served as a membrane-bound FRET acceptor. PKA holoenzymes are anchored in the cytosol to cytoskeletons via AKAPs at rest. In the presence of cAMP, PKA-C (labeled as "C") is released from PKA-R (R). When PKA-C becomes associated with membrane, there will be a decrease in distance between EGFP (G), which is tagged to PKA-C, and MARCKS-mCherry, leading to an increase in FRET and a corresponding decrease in EGFP lifetime. (B) Image of MARCKS-mCherry corresponding to the upper left panel of Figure 3C. The distribution of MARCKS-mCherry does not correlate with the apparent clusters in the lifetime map of Figure 3C, indicating that the distribution of MARCKS-mCherry is not the origin of the apparent clusters. (C) A simulation experiment showing the origin of the clustering noise in the upper left panel of Figure 3C. 50 photons were assigned to every pixel in a neuronal mask from the upper left panel of Figure 3C. The

arrival time of each photon was stochastically assigned following a probabilistic single exponential lifetime distribution with τ = 2.6 ns. The resulting simulated fluorescent lifetime map went through the same filtering and display procedures as those in Figure 3C. There are also apparent clusters in the image, indicating that the clusters in Figure 3C are due to noise in determining the fluorescent lifetime based on limited number of photons (~10-100 photons/pixel).

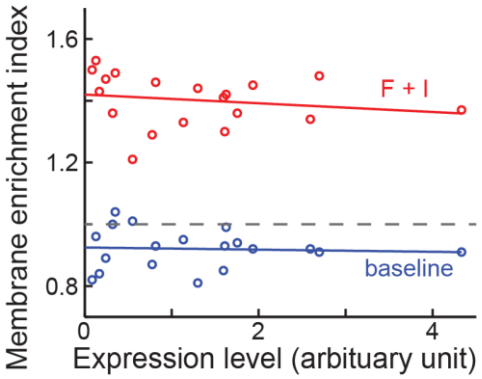

Figure S6. Related to Figure 3. Membrane enrichment indexes (MEI) are not dependent on the protein expression level.

PKA-C-EGFP was co-expressed with RIIβ and DsRed Express similar to Figure 3A. The measured MEIs for both baseline and forskolin/IBMX stimulated conditions are respectively correlated with the expression levels. The linear fits extrapolate to zero overexpression level at 0.92 and 1.42, respectively, for baseline and stimulated conditions. The gray dash line indicates even distribution.

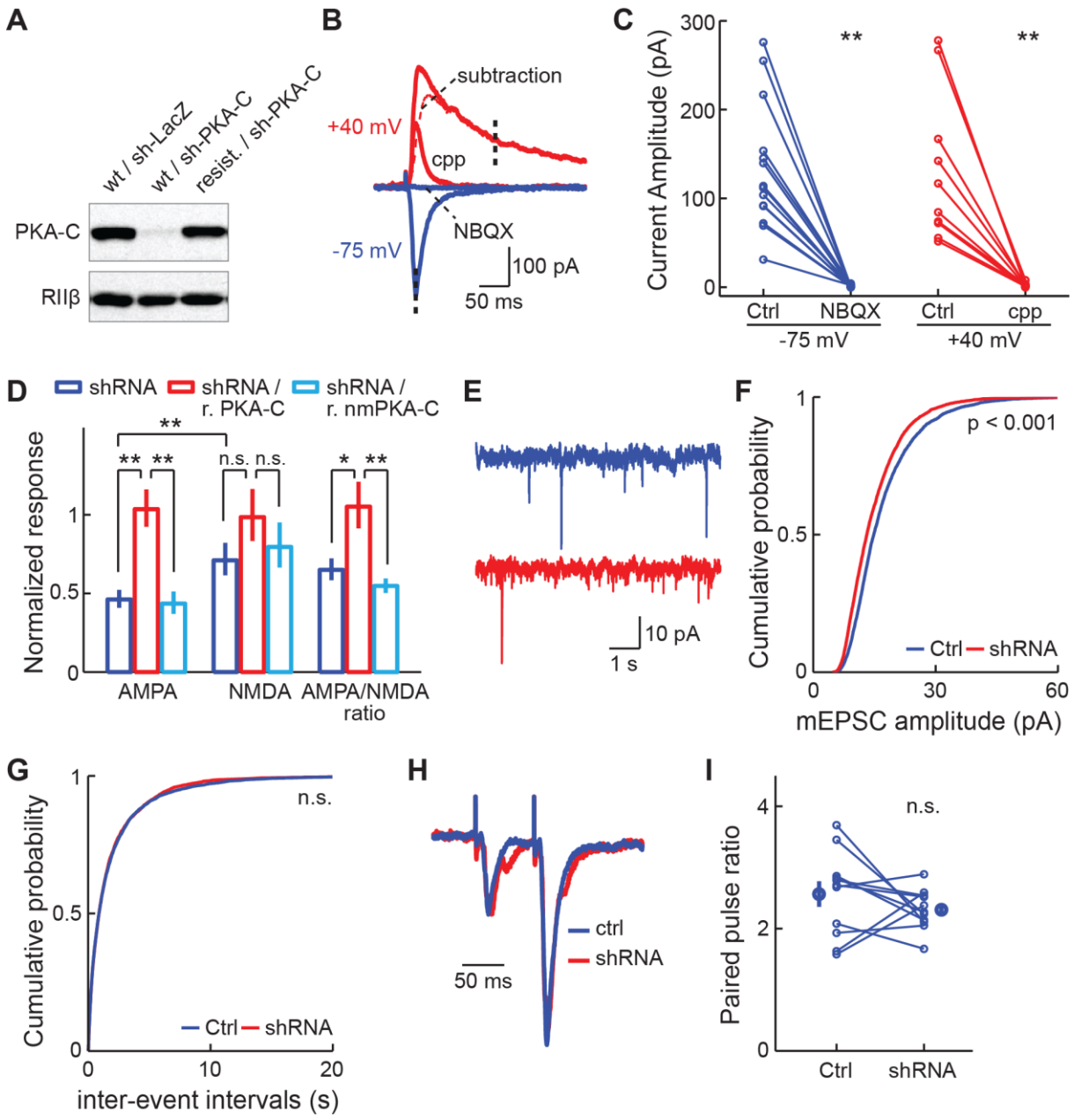

Figure S7. Related to Figure 7. Control experiments for the PKA-C knockdown and rescue experiment.

(A) A shRNA construct can effectively knock down wildtype but not the corresponding resistant PKA-C. Wildtype or shRNA-resistant (resist.) PKA-C tagged by EGFP was co-expressed with PKA-RIIβ and shRNA construct against wildtype PKA-C (sh-PKA-C) in 293

cells, as indicated. The resulting PKA-C and PKA-RIIβ expression was detected using an anti-EGFP and an anti-PKA-RIIβ antibody, respectively. sh-LacZ is a control shRNA targeting the irrelevant bacterial protein LacZ. (B, C) Example traces (B) and collective results (C) for AMPA (blue) and NMDA (red) receptor current measurements and their validations using specific antagonists. Thick dash lines indicate where the amplitudes are measured: AMPA amplitudes are measured as the peak evoked response at -75 mV holding potential; NMDA amplitudes are measured at +40 mV as the mean current at 140-160 ms after stimulation. The voltages are after correction of the junction potential. Both currents are sensitive to their respective antagonists: cpp blocks NMDA currents and NBQX blocks AMPA currents. Average current amplitudes are: AMPA, -134 ± 19 pA before NBQX, and -1.3 ± 0.3 pA after NBQX, n = 14; NMDA, 131 ± 26 pA before cpp, and 2.2 ± 0.7 pA after cpp, n = 10. (D) Geometric average of AMPA receptor currents, NMDA receptor currents, and AMPA/NMDA current ratios of CA1 neurons transfected with the indicated shRNA and rescuing constructs normalized to their paired, adjacent untransfected controls. The same electrical stimulation strength was applied to both sequentially recorded neurons of a pair. For all groups, n = 15 for shRNA, n = 18 for shRNA/r.PKA-C, and n = 15 for shRNA/r.nmPKA-C. (E, F, G) Representative traces (E) and cumulative probability plots for mEPSC amplitudes (F) and inter-event intervals (G) of CA1 neurons transfected with the shRNA construct and their paired, untransfected controls. Significance test was the Kolmogorov-Smirnov test. Median mEPSC amplitudes are 14.9 pA for control and 13.2 pA for shRNA knockdown. (H, I) Paired pulse current ratio of CA1 neurons transfected with shRNA construct against PKA-C (shRNA) and their paired, adjacent untransfected controls (ctrl). Average ratios are: 2.6 ± 0.2 for control, and 2.3 ± 0.1 for transfected neurons, n = 11.

SUPPLEMENTAL EXPERIMENTAL PROCEDURES

Plasmid constructs

Constructs were made using standard mutagenesis and subcloning methods. PKA-C-EGFP, PKA-C-paGFP, PKA-RIIβ and PKA-RIIβ-Δ2-5 have been previously described (Zhong et al., 2009). PKA-RIIβ-sREACh was constructed by replacing EGFP in PKA-RIIβ-EGFP with sREACh (Murakoshi et al., 2008) using PCR based subcloning with specific primers. PKA-Cn-paGFP was generated by deleting the sequence from position 48 to the end of PKA-C from PKA-C-paGFP. "nm" (non-myristoylated) PKA-C constructs were generated by mutating the glycine residue at position 2 to alanine. mCherry-histone 2b was purchased from Addgene. EGFP-GluA1 has been previously described (Shi et al., 1999). EGFP-GluA1c was generated by deleting the sequence between the position immediate after EGFP and the end of transmembrane domains. CD4-EGFP-GluA1c was constructed by replacing the entire intracellular portion of the human CD4 protein with EGFP-GluA1c. In MARCKS-paGFP and MARCKS-mCherry, only the N-terminal myristoylation and basic residue motif (the first 49 residues) of MARCKS were used.

AKAR5 was constructed from AKAR4 (Depry et al., 2011) independent of that recently published (Chen et al., 2014). We replaced monomeric Cerulean (Rizzo et al., 2004) with monomeric EGFP (Zacharias et al., 2002) and cp-Venus (Nagai et al., 2002; Nagai et al., 2001; Nagai et al., 2004) with sREACh or cp-sREACh to yield AKAR5 or AKAR5' respectively. cp-sREACh was generated using PCR primers so that a new start methionine was followed by residues 174 to 238 of sREACh and then in frame by residues 1 to 172 of sREACh with the linker GGTGGS. The leucine-rich nuclear export sequence of Mitogen-activated protein/extracellular signal-regulated kinase kinase (MEK) (LQKKLEELELDE)

(Fukuda et al., 1996) or the membrane-targeting farnesylation modification sequence from KRas (GKKKKKKSKTKCVIM) (Hancock et al., 1989) were introduced at the 3' terminus of AKAR5 and AKAR5' in separate constructs to generate cyt-AKAR5, m-AKAR5 and m-AKAR5'.

sh-PKA-C construct targeting the PKA-C DNA sequence AA CTT GAA TTC TCC TTC AA was generated using the EF1Ub-300 EGFP vector, which also express EGFP. To generate shRNA resistant PKA-C mutants, the above sequence was silently mutated into AG CTG GAG TTT TCT TTT AA.

Cell cultures, transfection and sample collection

HEK 293 cells were cultured in DMEM plus 10% fetal calf serum, penicillin-streptomycin and L-glutamine at 37°C and 5% CO2. Cells were plated on coverslips coated with Poly-D-Lysine, and transient transfections were performed using Lipofectamine 2000 (Invitrogen), according to the manufacturer's instructions. Cells were serum starved for 2 – 4 hours prior to imaging.

To compare two cell populations transfected with different reporter constructs, two plates of cells were differently transfected. One of the plates of cells received the red nucleus marker mCherry-histone2b in addition to the reporter constructs. 16 hours later, cells were trypsinized and harvested in complete medium. Equal numbers of cells from the two groups were mixed and re-plated onto coated cover slips and imaged the next day.

HEK 293 cells were transiently transfected with the indicated constructs. At 24 hours post transfection, cells were serum-starved overnight and then treated with 1μM NE

or 20 μM forskolin and 100 μM IBMX for 10min or the indicated times. For Figures 6B and 7, cells were then harvested, lysed and sonicated in ice cold lysis buffer containing (in mM) 150 NaCl, 50 NaF, 10 NaH_2PO_4, 5 EDTA,5 EGTA, 10 sodium pyrophosphate,1 sodium vanadate, plus 10 U/ml aprotinin and 1 μM okadaic acid and then centrifuged. The supernatant was mixed with equal amount of sample buffer containing 20% glycerol, and 10% beta-mercaptoethanol and 4% SDS in Tris-HCl buffer, and boiled for 5 min. For other figures where whole cell lysates were involved, the cells were lysed, harvested and sonicated directly in 1X Laemmli protein sample buffer.

Primary cortical neuronal cultures were prepared from E18 rat embryos following the protocol described (Xu et al., 2010) with the exception of substituting GS21 neural supplement (MTI-GlobalStem) for B27. Dissociated neurons were electroporated with plasmids expressing the indicated proteins using an Amaxa electroporator before plating. Neuronal whole-cell lysates were collected at DIV 14 after indicated treatments for 10 minutes within culture incubator and then subjected to western blotting analyses.

Co-immunoprecipitation

After serum starvation and indicated treatments, cells were lysed in IP buffer containing 1X PBS, 3 mM EDTA, 1% Triton X-100, 0.1 mM phenylmethanesulfonylfluoride (PMSF) and 1X Aprotinin (Sigma A6279 as 1000X), sonicated briefly with a probe type sonicator and spun at >100,000 g for 10 min. The soluble fraction was incubated with magnetic protein G beads (Life Technologies Novex 10007D) pre-incubated with a home-made mouse monoclonal anti-GFP antibody (clone# 4CQ, gift from Dr. Peter Barr-Gillespie, Vollum Institute) for 1 hour at room temperature. The beads were washed 1X with IP buffer, 2X

with IB buffer plus 500 mM NaCl, and then 2X with IP buffer. The precipitate was eluted with 1X Laemmli buffer and subjected to western analysis.

Western blotting analysis

The samples were run on either 7% fixed or 7 – 10% gradient polyacrylamide gels. The gels were then transferred overnight to PVDF membranes at 20V overnight or at 100V for two hours, and subjected to western blotting analyses using the indicated primary antibody and appropriate secondary antibodies. Used antibodies: anti-phospho-GluA1 (S485) (#AB5849) and anti-GluA1 (#05-855R) were from EMD Millipore, anti-GFP (#SC-8384) and anti-PKA-RIIβ (#SC-25424) were from Santa Cruz Biotechnology Inc, and anti-PKA-NT (#P9102-91A) were from US Biological. The anti-GFP antibody was used to detect the expression of EGFP-AKAP5 and, in Figure 7A, the expression of PKA-C-EGFP. In other figures, PKA-C was detected using the anti-PKA-NT antibody. In Figure 6B, 6C, 6J, 6K and 6L, western blot signals were detected with a LI-COR Odyssey scanner using the appropriate fluorescent secondary antibodies. In other western blots, chemiluminescent signals were first exposed to films before being scanned into computer. Under our conditions, the results between the two methods were qualitatively equivalent.

Two-photon imaging, photoactivation and uncaging

We use a custom built two-photon imaging setup based on an Olympus BW51WI microscope body. Two different laser beams (Maitai, Newport) were aligned and fed into the light path for simultaneous two-photon excitation and stimulation. Laser intensities were controlled by Pockels cells (Conotpics). Laser scanning was controlled by the ScanImage software (Pologruto et al., 2003). Slices were perfused in gassed artificial

cerebral spinal fluid (ACSF) containing 4 mM Ca, 4 mM Mg and 0.5 μM TTX during imaging. For the photoactivation experiments we used 810-nm excitation to focally photoactivate paGFP and 990 nm light from a separate laser to simultaneously image the photoactivated paGFP and the soluble mCherry marker of neuronal morphology. Spines were imaged for ~10 s at 4 or 8 Hz, with a pixel size of 60 – 100 nm and a field of view of ~ 6 μm. Power for photoactivation was determined empirically at the time of individual experiments. For glutamate uncaging experiments in Figure 7, 2.25 mM MNI-caged-L-glutamate (Tocris) was added to ACSF containing 4 mM calcium, 0.05 mM magnesium, 1 uM TTX and 4 μM 2-chloroadenosine as previously described (Harvey et al., 2008b). To trigger structural plasticity, 30 pulses of 4-ms 16-mW (at back focal plane) 720-nm laser light were delivered to the spine head at 0.5 Hz.

Two-photon fluorescence lifetime imaging (2pFLIM) and analyses

We used 960 nm to excite the donor fluorophore (monomeric EGFP) in the AKAR5 probes. The fluorescence of EGFP and other fluorophores, such as mCherry, at different wavelengths were unmixed using a dichroic mirror (Chroma 565DCXR) and band-pass filters (Chroma ET500/40x barrier filter for green and Semrock FF01-630/92 for red). Laser scanning was controlled by ScanImage. Fluorescence decay curves were measured in the time domain by comparing the arrival of the laser pulses detected by photodiode to the arrival of donor emitted photons detected by a fast photomultiplier tube using a TCSPC-730 time-correlated single photon counting board as previously described (Yasuda et al., 2006). Data acquisitions were performed by custom software in MATLAB kindly provided by Dr. Ryohei Yasuda with modification. Data analyses were performed using custom software written in MATLAB.

For Figures 3D and 5, because multiple populations of binding states exist within the sensor, or because the acceptor concentration was variable, measuring the binding ratio between the donor and acceptor fluorophores was not possible. We therefore report the mean photon emission time as an approximation of the fluorescence lifetime (Harvey et al., 2008a).

Electrophysiology

Whole-cell voltage-clamp recordings were performed using a MultiClamp 700B amplifier (Molecular Devices). Electrophysiological signals were filtered at 2 kHz and digitized and acquired at 20 kHz with custom software written in MATLAB. Slices were perfused with artificial cerebrospinal fluid containing 4 mM Ca and 4 mM Mg. The internal solution contained (in mM) 132 Cs-gluconate, 10 HEPES, 10 Na-phosphocreatine, 4 MgCl2, 4 Na2-ATP, 0.4 Na-GTP, 3 Na-ascorbate, 3 QX314, 0.2 EGTA with an osmolarity of 295 mOsmol/kg. The junction potential was calculated to be -17 mV using a built-in function in the Clampfit software (Molecular Devices). Several less abundant anions (phosphocreatine, ATP, GTP and ascorbate) were omitted in the calculation due to lack of data in the program. Cl reversal potential was -75 mV.

To reduce recurrent activities, cultured hippocampal slices were cut on both sides of CA1 and 4μM 2-chloroadenosine (Sigma) was present in all recording experiments. 10 μM GABAzine (SR 95531, Tocris) was also included to suppress GABA currents. For electrical stimulation, a bipolar, θ-glass stimulating electrode was positioned in the stratum radiatum 100–150 μm lateral to the recorded neuron. For all recordings, a transfected and an untransfected neuron within 50 μm from each other were sequentially recorded without

repositioning the stimulation electrode. Measurements were carried out on averaged traces from approximately 5 trials under each condition for AMPA/NMDA current ratio measurements and 10 trials for PPR. For mEPSC measurements, 1 μM TTX, 5 μM cpp and 10 μM GABAzine were included in the bath without cutting.

Image analysis for MEI measurements and photoactivation experiments

Image analysis was performed using custom software written in MATLAB. For MEI measurements, line profiles of five-pixel width were manually drawn across the apical dendrites that were larger than 1.8 μm in diameter and were smooth on both sides (i.e., void of spines). The profiles were obtained from a single optical section centered along the middle z-plane of the dendrite. The background subtracted fluorescence intensity in the green (from EGFP) and red (from DsRed) channel were then used to calculate the MEI. For SEI measurements, only the spines well isolated from the dendrite laterally throughout the entire experiments were included.

Photoactivation experiments were analyzed by manually drawing ROIs over the x – y projection of the spines of interest. The green fluorescence emission from the ROI over the course of the experiment was then averaged after subtracting the background value calculated from a manually drawn background ROI at the same frames. Only spines that show an activation signaling more than 3 times of the standard deviation of the background fluorescence fluctuation was included in data analysis. The green fluorescence intensity decays post photoactivation were then averaged across 3 separate trials and subsequently fit with a single exponential, the time constant of which were defined as the spine residence time.

SUPPLEMENTAL REFERENCES

Chen, Y., Saulnier, J.L., Yellen, G., and Sabatini, B.L. (2014). A PKA activity sensor for quantitative analysis of endogenous GPCR signaling via 2-photon FRET-FLIM imaging. Front Pharmacol *5*, 56.

Depry, C., Allen, M.D., and Zhang, J. (2011). Visualization of PKA activity in plasma membrane microdomains. Mol Biosyst *7*, 52-58.

Fukuda, M., Gotoh, I., Gotoh, Y., and Nishida, E. (1996). Cytoplasmic localization of mitogen-activated protein kinase kinase directed by its NH2-terminal, leucine-rich short amino acid sequence, which acts as a nuclear export signal. J Biol Chem *271*, 20024-20028.

Hancock, J.F., Magee, A.I., Childs, J.E., and Marshall, C.J. (1989). All ras proteins are polyisoprenylated but only some are palmitoylated. Cell *57*, 1167-1177.

Harvey, C.D., Ehrhardt, A.G., Cellurale, C., Zhong, H., Yasuda, R., Davis, R.J., and Svoboda, K. (2008a). A genetically encoded fluorescent sensor of ERK activity. Proc Natl Acad Sci U S A *105*, 19264-19269.

Harvey, C.D., Yasuda, R., Zhong, H., and Svoboda, K. (2008b). The spread of Ras activity triggered by activation of a single dendritic spine. Science *321*, 136-140.

Murakoshi, H., Lee, S.J., and Yasuda, R. (2008). Highly sensitive and quantitative FRET-FLIM imaging in single dendritic spines using improved non-radiative YFP. Brain Cell Biol *36*, 31-42.

Nagai, T., Ibata, K., Park, E.S., Kubota, M., Mikoshiba, K., and Miyawaki, A. (2002). A variant of yellow fluorescent protein with fast and efficient maturation for cell-biological applications. Nat Biotechnol *20*, 87-90.

Nagai, T., Sawano, A., Park, E.S., and Miyawaki, A. (2001). Circularly permuted green fluorescent proteins engineered to sense Ca2+. Proc Natl Acad Sci U S A *98*, 3197-3202.

Nagai, T., Yamada, S., Tominaga, T., Ichikawa, M., and Miyawaki, A. (2004). Expanded dynamic range of fluorescent indicators for Ca2+ by circularly permuted yellow fluorescent proteins. Proc Natl Acad Sci U S A *101*, 10554-10559.

Pologruto, T.A., Sabatini, B.L., and Svoboda, K. (2003). ScanImage: Flexible software for operating laser-scanning microscopes. BioMedical Engineering OnLine *2*, 13.

Rizzo, M.A., Springer, G.H., Granada, B., and Piston, D.W. (2004). An improved cyan fluorescent protein variant useful for FRET. Nat Biotechnol.

Shi, S.H., Hayashi, Y., Petralia, R.S., Zaman, S.H., Wenthold, R.J., Svoboda, K., and Malinow, R. (1999). Rapid spine delivery and redistribution of AMPA receptors after synaptic NMDA receptor activation. Science *284*, 1811-1816.

Xu, J., Xiao, N., and Xia, J. (2010). Thrombospondin 1 accelerates synaptogenesis in hippocampal neurons through neuroligin 1. Nat Neurosci *13*, 22-24.

Yasuda, R., Harvey, C.D., Zhong, H., Sobczyk, A., van Aelst, L., and Svoboda, K. (2006). Supersensitive Ras activation in dendrites and spines revealed by two-photon fluorescence lifetime imaging. Nat Neurosci *9*, 283-291.

Zacharias, D.A., Violin, J.D., Newton, A.C., and Tsien, R.Y. (2002). Partitioning of lipid-modified monomeric GFPs into membrane microdomains of live cells. Science *296*, 913-916.

Zhong, H., Sia, G.M., Sato, T.R., Gray, N.W., Mao, T., Khuchua, Z., Huganir, R.L., and Svoboda, K. (2009). Subcellular dynamics of type II PKA in neurons. Neuron *62*, 363-374.